ORIGIN OF PRECIPITATE-FREE ZONES IN AL-MN-FE ALLOYS

C. Sigli
Pechiney Centre de Recherches de Voreppe,
B.P. 27 - 38340 Voreppe - France

Abstract

A model has been developed to describe the precipitation of Mn and Fe during solidification and heat treatment of ternary Al-Mn-Fe alloys. The model explains the formation, during homogenizing, of precipitate-free zones (PFZ) on the periphery of the dendrites.

A Scheil-Gulliver model is used to simulate the Fe and Mn microsegregation gradients within dendrites, predicting a strong manganese depletion on the dendrite periphery. This prediction is confirmed experimentally.

During homogenizing, diffusion inside the dendrites is described numerically by a finite-difference method. An example of calculation is given for the ternary Al-1.08wt%Mn-0.48wt%Fe alloy. After 8h at 620°C, the volume fraction of the precipitate-free zone is predicted to be equal to 49%; this prediction is in good agreement with the measured volume fraction of 47±6 %.

Introduction

Al-Mn-Mg-(Fe,Si) alloys contain precipitate-free zones (PFZ) that develop at the periphery of dendrite arms after casting and homogenizing at sufficiently high temperature [1-8]. This non-uniform precipitate distribution is an important microstructural feature as it induces heterogeneities in the recrystallization kinetics and texture evolution during hot rolling [9,10,11,12]. In order to obtain minimum earing of the final products, texture evolution of flat rolled products can be optimized by controlling the volume fraction of the PFZ.

The origin of the PFZ is not fully understood and different explanations can be found in literature. P. Furrer invokes a depletion of manganese around primary particles by diffusion of manganese atoms toward primary particles during heat treatment [5]; on the other hand, T.H. Sanders explains this phenomenon in terms of the competing effects of magnesium segregation on the solubility of manganese and of manganese segregation on the availability of manganese to precipitate [8].

This paper presents an alternative explanation: it is shown that the presence of PFZ can be explained by an interaction between manganese and iron during solidification and heat treatment. A model is proposed in order to explain the origin of PFZ.

Experimental evidence of the role of Mn and Fe on the origin of PFZ

A ternary Al-1.08wt%Mn-0.48wt%Fe alloy has been cast in a 0.3 mm thick walled cylindrical mould with a diameter of 55mm. The iron and manganese alloy composition is close to that of the industrial AA3104 alloy. The average secondary dendrite arm spacing (SDAS) of the cast structure obtained by this procedure is approximately 90-100 μm. This spacing is slightly higher than the average SDAS measured in the center of a 600 mm thick AA3104 slab which is around 80 μm.

A microprobe mapping of the manganese concentration was performed on the as-cast sample and is shown in Fig.1. The mapping indicates a strong depletion of manganese on dendrite peripheries. This peculiar behavior is entirely due to the presence of iron in the alloy and is not observed in a binary Al-1wt% Mn.
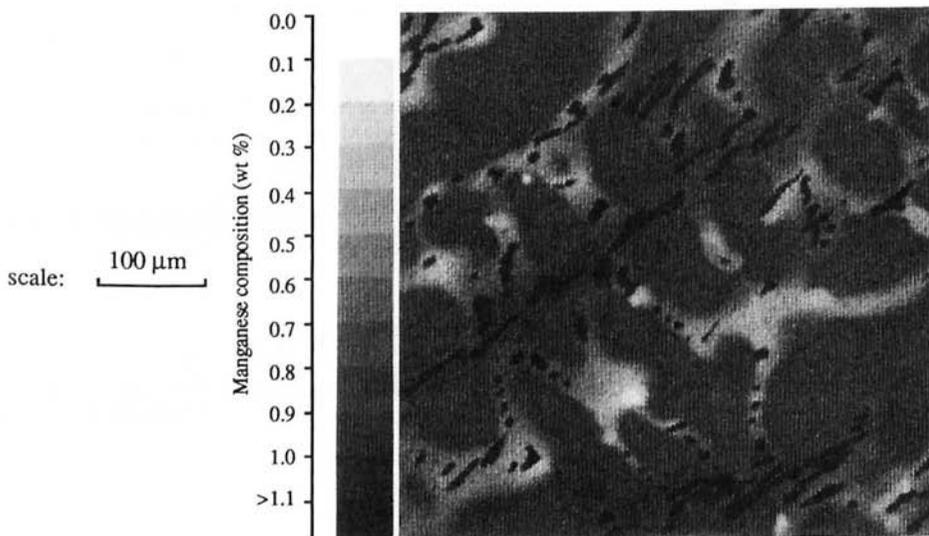

Figure 1. Manganese concentration in the as-cast Al-1.08wt%Mn-0.48wt%Fe alloy.

After casting the alloy was held at 620°C for 8 hours with a previous heating rate of 75°C/h. Micrographs were performed during the heat treatment and are presented in Fig.2. At the end of the heat treatment, precipitate-free zones can be distinguished. Their surface fraction, assumed to be equal to the volume fraction, was measured and found to be equal to 47±6 %. Also indicated in Fig.2 is the evolution of the average manganese concentration in the aluminum matrix measured by Thermo-Electrical Power (TEP) [13,14]: it increases with temperature above 550°C and remains approximately constant during the holding at 620°C for 8 hours. The method used to determine the manganese matrix concentration from TEP measurements is described elsewhere in these proceedings [15].

The two following sections present a theoretical explanation for these observations. The first one describes a model that predicts the iron and manganese concentration gradients within secondary dendrite arms after solidification; the second section presents a calculation of the PFZ volume fraction during homogenizing.
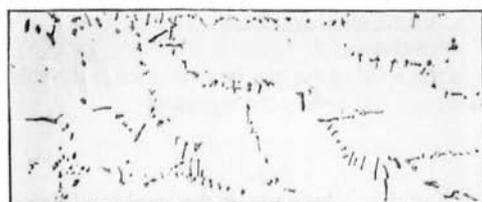
As-cast alloy,
Mn concentration in matrix = 0.72±0.02 wt %,
(TEP measurement : -304±2 10^{-8} V/°C).
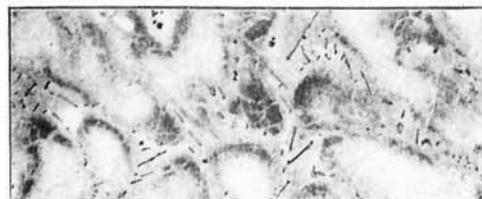
Heated up to 500°C at 75°C/s,
Mn concentration in matrix = 0.57±0.02 wt %,
(TEP measurement : -267±2 10^{-8} V/°C).
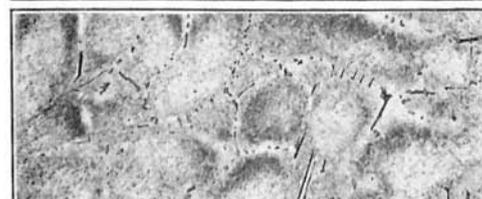
Heated up to 550°C at 75°C/s,
Mn concentration in matrix = 0.48±0.02 wt %,
(TEP measurement : -239±2 10^{-8} V/°C).

Heated up to 580°C at 75°C/s,
Mn concentration in matrix = 0.51±0.02 wt %,
(TEP measurement : -250±2 10^{-8} V/°C).

Heated up to 620°C at 75°C/s,
Mn concentration in matrix = 0.63±0.02 wt %,
(TEP measurement : -281±2 10^{-8} V/°C).

Heated up to 620°C at 75°C/s
+ 8h at 620°C,
Mn concentration in matrix = 0.62±0.02 wt %,
(TEP measurement : -279±2 10^{-8} V/°C).

⊢————⊣ : 200μm

Figure 2. Microstructural evolution of Al-1.08Mn-0.48Fe alloy during heat treatment

Simulation of the as-cast microstructure of Al-Mn-Fe alloys

During solidification, diffusion of solute atoms in the solid phase can be neglected if the solute back diffusion coefficient (α) is small. This coefficient is defined by the equation:

$$\alpha = \frac{4\,D_s\,t_f}{SDAS^2} \tag{1}$$

where D_s is the solid state diffusion coefficient of the solute atom and t_f is the local solidification time. In order to evaluate α, the variation of the SDAS with the local solidification has been supposed to be identical to that of AA3104:

$$SDAS = 4.25\,t_f^{0.39} \quad [16] \text{ (time in s, distance in } \mu m) \tag{2}$$

whereas the diffusion coefficient of the solute atoms are taken to be equal to :

$$D_s[Fe] = 53\ 10^8\ e^{-\frac{183.2\ (kJ/mole)}{RT}} \quad (\mu m^2/s) \quad [17] \tag{3.a}$$

$$D_s[Mn] = 104\ 10^8\ e^{-\frac{211.2\ (kJ/mole)}{RT}} \quad (\mu m^2/s) \quad [18] \tag{3.b}$$

For an SDAS of 100μm, corresponding to a local solidification time of 556 s (see Eq.2), and for a solidification temperature approximately equal to 658°C, the value of the back diffusion coefficient is indeed small and equal to 0.061 for iron and to 0.003 for manganese; diffusion of solute atoms in the solid phase can therefore be neglected for Al-Mn-Fe alloys.The same conclusion can be drawn from the results of Y. Langsrud [19].

The calculations of as-cast structure have been performed by assuming (Scheil model [20]):
- negligible diffusion of solute atoms in the solid phase,
- infinite diffusion of solute atoms in the liquid phase,
- that the local equilibrium at the solid-liquid interface is given by the Al-Mn-Fe phase diagram [21].

The calculated solidification path of the ternary Al-1.08wt%Mn-0.48wt%Fe alloy is shown in Fig.3.a together with the computed manganese and iron composition gradient within secondary dendrite arm (Fig.3.b). The strong manganese depletion on the dendrite periphery is explained by the alloy solidification path: as soon as the liquid concentration reaches the eutectic trough, the manganese concentration in the liquid and in the aluminum matrix is forced to decrease (see Fig.3). The predictions are, at least qualitatively, in good agreement with the microprobe mapping shown in Fig.1.

Simulation of the appearance of PFZ in Al-Mn-Fe alloys after homogenizing

The basic assumptions used in the calculation of the microstructure during heat treatment are :
- the matrix concentration gradient of one element is supposed not to affect the diffusion flux of the other element, i.e. the diffusion matrix is diagonal, the diagonal terms are given by Eq.3.a-b;
- a zero flux condition is applied at the periphery of secondary dendrite arms. This assumption is consistent with the TEP measurements which remain constant during the period at 620°C (see Fig.2);
- each volume element of a secondary dendrite arm is in the equilibrium state determined by the local iron and manganese composition and the ternary Al-Mn-Fe phase diagram [21] (see Fig.4).
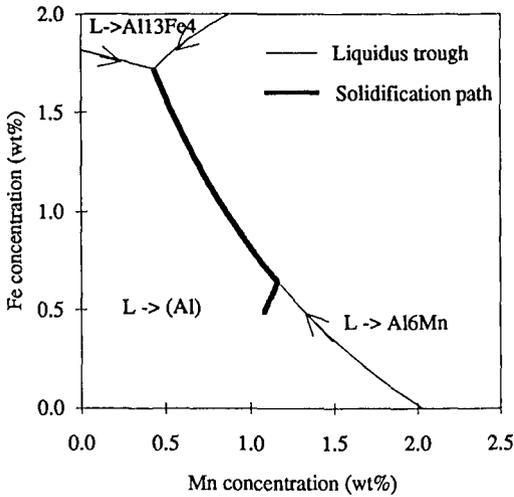
Figure 3.a Calculated solidification path for an Al-1.08wt%Mn-0.48wt%Fe alloy.
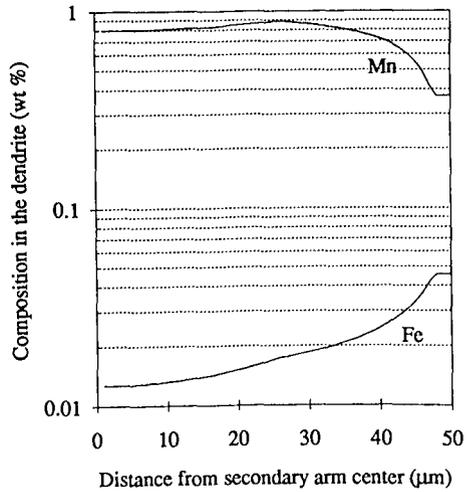
Figure 3.b Calculated composition gradients for an Al-1.08wt%Mn-0.48wt%Fe alloy.
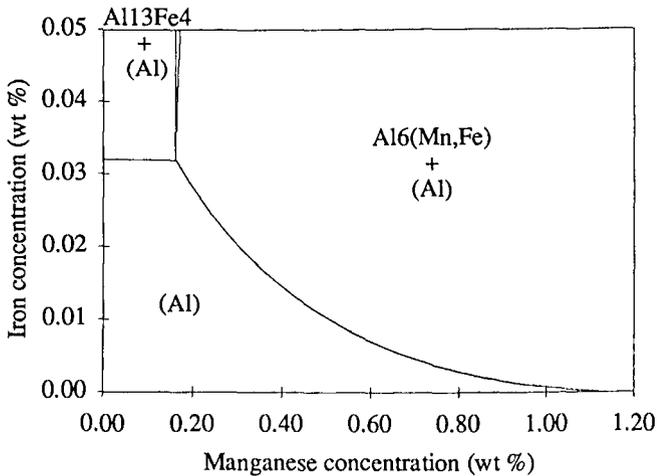
Figure 4: Al-Mn-Fe phase diagram at 620°C according to [21].

A finite difference method is used to solve Fick's second law of diffusion for iron and manganese. The computation scheme is presented in Fig.5. Fig.6 shows a result of the calculation: the evolution of the precipitate-free zone volume fraction as a function of holding time at 620°C. The size of the PFZ increases with time; after 8 hours, a PFZ volume fraction of 49% is calculated. This prediction is consistent with the measurement of 47±6%.

```
┌─────────────────────────────────────────────────────────────────────┐
│  ┌──────────────────────────────────────────────────────────┐        │
│  │ Read initial composition gradient of manganese and iron  │        │
│  │ calculated by the solidification model.                  │        │
│  └──────────────────────────────────────────────────────────┘        │
│                              │                                        │
│  ┌──────────────────────────────────────────────────────────┐        │
│  │ For each volume element in a secondary dendrite arm,     │        │
│  │ calculate the equilibrium microstructure given by the    │        │
│  │ phase diagram [21]:                                      │        │
│  │          - Fe and Mn matrix concentration ,             │        │
│  │          - mass fraction of dispersoids,                │        │
│  │          - composition of dispersoids.                  │        │
│  └──────────────────────────────────────────────────────────┘        │
│                              │                                        │
│  ┌──────────────────────────────────────────────────────────┐        │
│  │ After increment of time dt, solve Fick's second law and  │        │
│  │ calculate new Fe and Mn composition gradient.            │        │
│  └──────────────────────────────────────────────────────────┘        │
│                              │                                        │
│  ┌──────────────────────────────────────────────────────────┐        │
│  │ For each volume element in a secondary dendrite arm,     │        │
│  │ calculate the equilibrium microstructure given by the    │        │
│  │ phase diagram [21]:                                      │        │
│  │          - Fe and Mn matrix concentration ,             │        │
│  │          - mass fraction of dispersoids,                │        │
│  │          - composition of dispersoids.                  │        │
│  └──────────────────────────────────────────────────────────┘        │
└─────────────────────────────────────────────────────────────────────┘
```

Figure 5. Computation scheme for the prevision of precipitate-free zone formation .
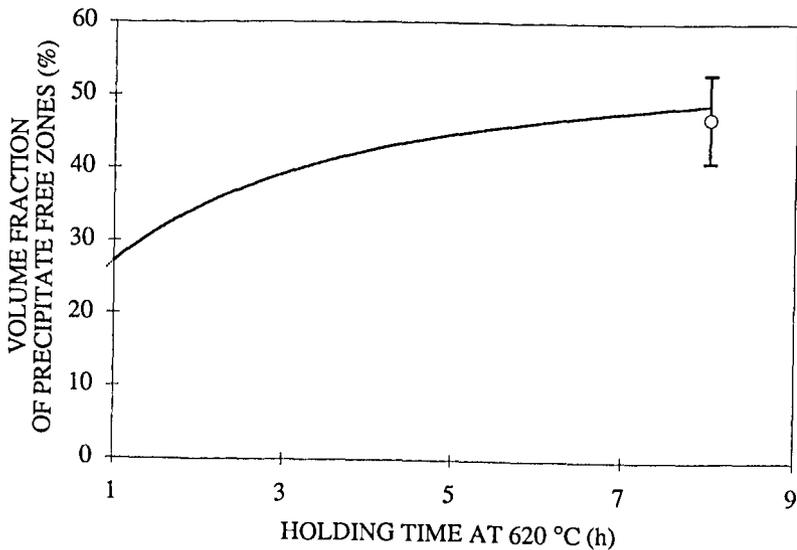
Figure 6. Evolution of precipitate free zone volume fraction as a function of time at 620°C.

Conclusion

The precipitate-free zones that develop during homogenizing of Al-Mn-Mg-Fe-Si alloys are due to the interaction of manganese and iron during solidification and heat treatment. After casting, a strong depletion of manganese appears on the dendrite periphery. This depletion is explained by the solidification path: when the liquid concentration follows the eutectic trough "L -> $Al_6(Mn,Fe)+(Al)$" the matrix concentration of manganese is forced to decrease.

During homogenizing at temperatures above 580°C, this composition profile together with the relative values of solute diffusivities induce the formation of precipitate-free zones on the dendrite periphery.

References

1. L.F. Mondolfo, Aluminium Alloys, Structure and Properties (London: The Butterworths Group, 1976), 836.

2. G.M. Raynaud, B. Grange and C. Sigli, Aluminium Alloys, Their Physical and Mechanical Properties vol III (Trondheim, Arnberg, Lohne, Nes and Ryum 1992), 169.

3. T. Sheppard and N. Raghunathan, Mat. Sci.& Techn. 5, (1989), 268.

4. J. Hatch, Aluminum properties and physical metallurgy (ASM, 1984), 65.

5. P. Furrer and G. Hausch, Metal Science, (1979), 155.

6. T. Doko, S. Asami and K. Yagi, J. Japan Inst. Light Metals 38, (1988), 386.

7. A.M. Sumner, Metallurgia and Metal Forming, (1973), 300.

8. T.H. Sanders, Jr., Metallography 14, (1981), 177.

9. T. Doko and S. Asami, Furukawa Review n°9, (1991), 41.

10. K. Fukada, M. Mizouchi and T. Kajiyama, Aluminium Alloys, Their Physical and Mechanical Properties vol I, (Charlottesville, E.A. Starke and T.H. Sanders, 1986), 483.

11. P.L. Morris and B.J. Duggan, Metal Science 12, (1978), 1.

12. D.J. Lloyd, Metal Science 16, (1982),304.

13. F.R. Boutin, S. Dermarkar and B. Meyer, Proc. 7th Light Metals Congress (Leoben 1981), 212.

14. R. Borrely, P. Merle and D. Adenis, Light Metals 1989 (Ed. By P.G. Campbell), 703.

15. C. Sigli, "Solubility limit of Mn and Si in Al-Mn-Si at 550°C", these proceedings.

16. T.Z. Kattamis, H.D. Merchant and G. Scharf, Homogeneization and Annealing of Aluminum and Copper Alloys, TMS (1988), 117.

17. D.L. Beke et al., Phil. Mag. A55, (1987), 425.

18. G.M. Hood and R.J. Schultz, Phil. Mag. 23, (1971), 1479.

19. Y. Langsrud, User Aspects of Phase diagrams (F.H. Hayes, The Institute of Metals 1991), 90.

20. E. Scheil, Z. Metallkd. 34, (1942), 70.

21. Åke Janson, private communication.